International Journal of Thermophysics (2022) 43:127
https://doi.org/10.1007/s10765-022-03052-7

Speed of Sound Measurements of Binary Mixtures of Hydrofluorocarbons [Pentafluoroethane (R-125), 1,1-Difluoroethane (R-152a), or 1,1,1,2,3,3,3-Heptafluoropropane (R-227ea)] with Hydrofluoroolefins [2,3,3,3-Tetrafluoropropene (R-1234yf) or *trans*-1,3,3,3-Tetrafluoropropene (R-1234ze(E))]

Aaron J. Rowane[1] · **Richard A. Perkins**[1]

Received: 26 May 2022 / Accepted: 30 May 2022 / Published online: 28 June 2022

Abstract

Speed of sound data measured using a dual-path pulse-echo instrument are reported for three binary refrigerant mixtures, R-125/1234yf, R-1234yf/152a, and R-1234ze(E)/227ea, at compositions of (0.33/0.67) and (0.67/0.33) mole fraction. The speed of sound was studied at temperatures ranging from 230 K to 345 K from pressures slightly above the bubble point curve up to 20 MPa for the mixtures containing R-1234yf and 49 MPa for the R-1234ze(E)/227ea mixtures. The relative combined expanded speed of sound uncertainty ranged from 0.039 % to 0.317 % with a mean uncertainty over all state points of less than 0.10 %. The reported data are compared to the most recent mixture models in REFPROP for each blend studied. Comparisons of available mixture models for the R-125/1234yf and R-1234yf/152a blends exhibit average absolute deviation values ranging from 0.10 % to 0.27 %, and the average absolute deviations for R-1234ze(E)/227ea blends range from 0.62 % to 0.94 %. The comparisons show that only minor adjustments are required to the R-125/1234yf and R-1234yf/152a mixture models to represent the speed of sound data within its uncertainty. However, significant adjustments are needed to improve the current mixture models for the R-1234ze(E)/227ea blend. Deficiencies with the R-1234ze(E)/227ea mixture model are not unexpected since it (1) utilizes a pure-fluid EOS R-1234ze(E) that has been shown to inaccurately represent R-1234ze(E)

Commercial equipment, instruments, or materials are identified only to adequately specify certain procedures. Such identification does not imply recommendation or endorsement by the National Institute of Standards and Technology, nor does it imply that the identified products are necessarily the best available for the purpose. Contribution of the National Institute of Standards and Technology; not subject to copyright in the United States.

Extended author information available on the last page of the article

speed of sound values and (2) uses binary interaction parameters for the chemically similar mixture of R-1234yf/227ea.

Keywords Hydrofluorocarbons · Hydrofluoroolefins · REFPROP · Refrigerant mixtures · R-125 · R-152a · R-227ea · R-1234yf · R-1234ze(E) · Speed of sound

1 Introduction

The next generation of refrigerants are expected to be mixtures of hydrofluorocarbons (HFC) and hydrofluoroolefins (HFO) to meet toxicity, flammability, ozone depletion potential (ODP), global warming potential (GWP), and performance constraints. A database of accurate refrigerant thermophysical properties enables the integration of new low GWP refrigerants into current and future refrigeration systems. The present study expands on a larger project from our group which reports bubble point [1, 2], speed of sound [3, 4], density, thermal conductivity, and viscosity data for several binary mixtures of HFC and HFO refrigerants. The thermophysical property data generated by our group have been used by Bell [5] to improve mixture models for several blends of HFCs and HFOs. The present study expands on this effort and reports speed of sound data for R-125/1234yf, R-1234yf/152a, and R-1234ze(E)/227ea mixtures at nominal compositions of (0.33/0.67) and (0.67/0.33) mole fraction. The data are reported at temperatures ranging from 230 K to 345 K and from pressures just above the bubble point pressure to 20 MPa for blends with R-1234yf and 49 MPa for R-1234ze(E)/227ea blends. The data from the present study are used to assess the performance of mixture models currently in REFPROP [6] for each blend investigated. The mixture models included in REFPROP are constructed from pure-fluid equations of state (EOS) [7–11] for each blend component and binary interaction parameters [12, 13].

2 Materials and Methods

The sample preparation, dual-path pulse echo, and loading and isochoric measurement procedure used in this study are identical to those reported in previous studies [3, 4, 14]. Therefore, only brief descriptions are provided here, and the reader is referred to our previous work for more detail.

2.1 Sample Preparation

Table 1 lists the refrigerants used in this study along with their short names, CAS numbers, molar mass, source, and purity. As described in our previous studies, [3, 4] degassed pure-component samples were used to prepare vapor-phase samples of each mixture. All mixtures were prepared gravimetrically using the double-substitution method of Harris and Torres [15]. The composition's estimated standard uncertainty was less than 0.00005 mole fraction when considering contributions

Table 1 Refrigerant samples used in this study listed with their CAS numbers, molar mass, source, and purity

Chemical name	CAS Number	Molar Mass/ ($g \cdot mol^{-1}$)	Source	Purity/mole percent
Pentafluoroethane (R-125)	354–33-6	120.02	Scott Specialty Gas	99.99
1,1-difluoroethane (R-152a)	75–37-6	66.05	Chemours	99.9355
1,1,1,2,3,3,3-heptafluoropropane (R-227ea)	431–89-0	170.03	Honeywell	99.97
2,3,3,3-tetrafluoropropene (R-1234yf)	754–12-1	114.04	Chemours	99.9
1,3,3,3-*trans*-tetrafluoropropene (R-1234ze(E))	29,118–24-9	114.04	Honeywell	99.97

All samples were degassed using a freeze–pump–thaw method prior to preparing mixtures and the sample purity was confirmed by gas chromatography

from gravimetric preparation, potential contamination of the outside of the sample cylinder with dirt or dust, sorption of sample onto the inner cylinder walls and filling valves, and expansion of the cylinder when filled. The largest contribution to the sample uncertainty was associated with the impurities in the components used to prepare each mixture. The fraction of the impurity for each component was considered in the final composition standard uncertainty by adding it in quadrature with the estimated standard uncertainty from all the aforementioned sources. Table 2 lists the compositions, total sample masses, and standard uncertainties in the composition for each mixture prepared.

2.2 Dual-Path Pulse-Echo Instrument

The dual-path pulse-echo instrument used in this study is identical to that described in our previous studies. Therefore, only selected details are restated here and the interested reader is referred to our previous studies [3, 4, 14] for more information.

Table 2 Mixture compositions for the studied binary mixtures listed with total sample mass prepared and standard mole fraction uncertainties

Mixture	Composition/mole frac	Sample Mass/g	$u_c(x_1)$/mole frac
R-125/1234yf	(0.33351/0.66649)	319.5556	0.00067
R-125/1234yf	(0.66643/0.33357)	344.6452	0.00034
R-1234yf/152a	(0.33342/0.66658)	281.4816	0.00070
R-1234yf/152a	(0.66526/0.33474)	306.3078	0.00055
R-1234ze(E)/227ea	(0.33265/0.66735)	378.4553	0.00023
R-1234ze(E)/227ea	(0.66803/0.33197)	355.0070	0.00023

The dual-path pulse-echo instrument used in this study had a temperature range from 230 K to 423 K and could operate to a maximum pressure of 70 MPa. The standard uncertainties of the temperature and pressure were 0.004 K and 0.014 MPa, respectively. The relative combined expanded uncertainty of the speed of sound for the present measurements ranged from 0.039 % to 0.317 % with an average uncertainty of less than 0.10 %. The speed of sound uncertainty increased as the state point approached the blend's mixture critical point where lower sound velocities and weaker echo signals were encountered.

2.3 Loading and Isochoric Measurement Procedure

The measuring cell was cooled to 228 K and was then filled by condensing in vapor-phase sample from the supply cylinder until the cell was liquid filled. A majority of the filling manifold, which was at room temperature of 293 K, remained vapor filled immediately following the filling procedure. Measurements commenced at 230 K and a pressure near the saturation pressure; the temperature was increased in 5 K increments, and this caused the liquid to expand into the filling manifold. Once the filling manifold was completely filled with liquid, the pressure would increase by several MPa with each increment in temperature, and this terminated at what we call the "near-saturation trace." Measurements then proceeded along pseudo-isochores with temperature incremented in 5 K steps until the maximum desired pressure was reached. The pressure was then reduced to a pressure 0.5 MPa above the bubble point determined using the available mixture models in REFPROP [6]. This process was repeated by dropping to a temperature 5 K above the starting temperature of the previous isochore. Up to twelve speed of sound data points were obtained at each state point where measurements were performed. It is important to note that in previous studies [3, 4], pressures for mixtures with R-1234yf were limited to 12 MPa to avoid potential polymerization reactions. However, in the present study, no noticeable polymerization occurred at pressures up to 20 MPa and repeated speed of sound measurements showed no change in the measured speed of sound values.

3 Results and Discussion

The following sections report the experimental speed of sound data measured using the dual-path pulse-echo instrument. The new speed of sound data is then compared to mixture models included in REFPROP, and their performance is discussed.

3.1 Experimental Speed of Sound Data

Figure 1a to f show the relationship between the speed of sound and temperature for the measured *T*-*w* points from pressures slightly above the bubble point pressure and several pseudo-isochores for the R-125/1234yf, R-1234yf/152a, and R-1234ze(E)/227ea mixtures. Only every other isochore for each mixture is shown in Figure 1a to f to avoid clutter on the plots. Density labels for each pseudo-isochore are averaged REFPROP

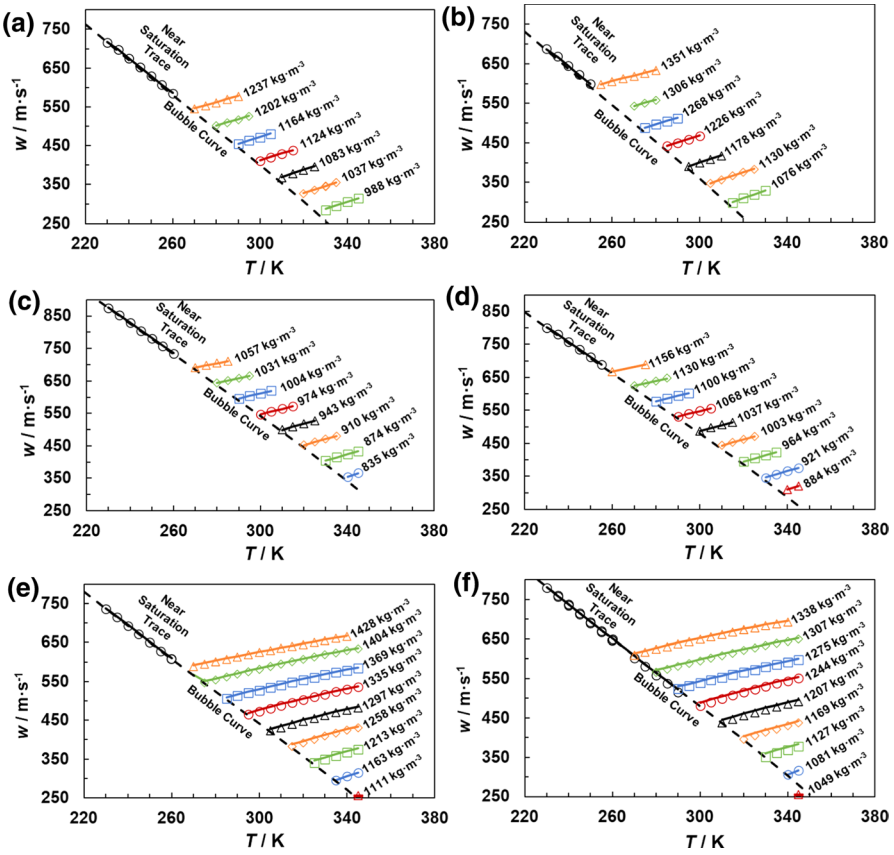

Fig. 1 Relationship between the speed of sound and temperature for binary mixtures of hydrofluorocarbons (R-125, R-152a, or R-227ea) with hydrofluoroolefins (R-1234yf or R-1234ze(E)) along several pseudo-isochores. The systems and molar compositions are (a) R-125/1234yf (0.33351/0.66649), (b) R-125/1234yf (0.66643/0.33357), (c) R-1234yf/152a (0.33342/0.66658), (d) R-1234yf/152a (0.66526/0.33474), (e) R-1234ze(E)/227ea (0.33265/0.66735), and (f) R-1234ze(E)/227ea (0.66803/0.33197). Symbols represent experimental data points while lines represent predictions with REFPROP [6] along the nominal density; for clarity, only every other isochore is shown

values calculated using the measured temperatures and pressures at each state point along a given psuedo-isochore. Lines drawn on each plot are speed of sound values calculated with REFPROP [6]. REFPROP implements the pure-fluid EOS of Lemmon and Jacobson [10] for R-125, Outcalt and McLinden [11] for R-152a, Lemmon and Akasaka [7] for R-1234yf, Thol and Lemmon [8] for R-1234ze(E), and Lemmon and Span [9] for R-227ea. The binary interaction parameters for R-125/1234yf are reported by Bell et al. [13], and for R-1234yf/152a by Bell and Lemmon [12]. No binary interation parameters are available for the R-1234ze(E)/227ea blend, and therefore, parameters for the R-1234yf/227ea mixture of Bell and Lemmon [12] are used in this study. Tables 3, 4 and 5 list the temperature, pressure, speed of sound averaged from up to twelve measurements, and the relative combined expanded uncertainty of

Table 3 Experimental speed of sound data for the R-125/1234yf mixtures

x_1/mole frac	x_2/mole frac	$u_c(x_1)$/mole frac	T/K	p/MPa	w/m•s^{-1}	$U_c(w)$/ %
0.33351	0.66649	0.00067	229.997	0.107	716.21	0.044
0.33351	0.66649	0.00067	235.006	0.744	697.54	0.045
0.33351	0.66649	0.00067	240.002	0.803	675.15	0.047
0.33351	0.66649	0.00067	245.002	0.818	652.50	0.049
0.33351	0.66649	0.00067	250.004	0.825	629.84	0.052
0.33351	0.66649	0.00067	254.994	0.836	607.26	0.055
0.33351	0.66649	0.00067	259.986	0.849	584.75	0.059
0.33351	0.66649	0.00067	269.992	4.667	575.51	0.058
0.33351	0.66649	0.00067	274.995	7.870	582.88	0.055
0.33351	0.66649	0.00067	279.999	11.062	590.02	0.053
0.33351	0.66649	0.00067	269.990	4.084	570.31	0.059
0.33351	0.66649	0.00067	274.995	7.259	577.72	0.057
0.33351	0.66649	0.00067	279.999	10.444	585.08	0.054
0.33351	0.66649	0.00067	284.999	13.619	592.26	0.052
0.33351	0.66649	0.00067	269.989	1.474	545.69	0.066
0.33351	0.66649	0.00067	274.993	4.529	553.43	0.062
0.33351	0.66649	0.00067	279.998	7.594	561.08	0.059
0.33351	0.66649	0.00067	285.000	10.710	568.96	0.056
0.33351	0.66649	0.00067	290.001	13.780	576.34	0.053
0.33351	0.66649	0.00067	274.992	1.591	524.38	0.071
0.33351	0.66649	0.00067	279.998	4.500	532.30	0.067
0.33351	0.66649	0.00067	284.999	7.424	540.15	0.063
0.33351	0.66649	0.00067	290.002	10.348	547.79	0.060
0.33351	0.66649	0.00067	294.996	13.264	555.22	0.057
0.33351	0.66649	0.00067	279.996	1.536	501.19	0.078
0.33351	0.66649	0.00067	284.998	4.294	509.34	0.073
0.33351	0.66649	0.00067	290.000	7.065	517.35	0.068
0.33351	0.66649	0.00067	294.997	9.839	525.16	0.064
0.33351	0.66649	0.00067	284.998	1.500	477.98	0.086
0.33351	0.66649	0.00067	290.001	4.115	486.39	0.080
0.33351	0.66649	0.00067	294.997	6.738	494.59	0.074
0.33351	0.66649	0.00067	299.998	9.369	502.59	0.070
0.33351	0.66649	0.00067	290.000	1.462	454.43	0.096
0.33351	0.66649	0.00067	294.996	3.941	463.24	0.088
0.33351	0.66649	0.00067	299.998	6.425	471.71	0.082
0.33351	0.66649	0.00067	304.997	8.914	479.88	0.076
0.33351	0.66649	0.00067	294.994	1.527	431.92	0.107
0.33351	0.66649	0.00067	299.996	3.868	440.96	0.098
0.33351	0.66649	0.00067	304.997	6.217	449.66	0.090
0.33351	0.66649	0.00067	309.999	8.573	458.02	0.083
0.33351	0.66649	0.00067	299.995	1.727	411.00	0.119
0.33351	0.66649	0.00067	304.996	3.942	420.33	0.108

Table 3 (continued)

x_1/mole frac	x_2/mole frac	$u_c(x_1)$/mole frac	T/K	p/MPa	w/m•s^{-1}	$U_c(w)$/ %
0.33351	0.66649	0.00067	310.000	6.167	429.22	0.099
0.33351	0.66649	0.00067	314.993	8.391	437.71	0.091
0.33351	0.66649	0.00067	304.993	1.803	388.15	0.136
0.33351	0.66649	0.00067	309.997	3.882	397.71	0.122
0.33351	0.66649	0.00067	314.994	5.967	406.78	0.111
0.33351	0.66649	0.00067	320.004	8.057	415.38	0.102
0.33351	0.66649	0.00067	309.997	2.071	367.74	0.153
0.33351	0.66649	0.00067	314.991	4.030	378.01	0.137
0.33351	0.66649	0.00067	320.004	6.003	387.27	0.124
0.33351	0.66649	0.00067	325.009	7.977	396.01	0.113
0.33351	0.66649	0.00067	314.991	2.342	348.44	0.173
0.33351	0.66649	0.00067	320.002	4.183	357.97	0.154
0.33351	0.66649	0.00067	325.007	6.033	367.70	0.138
0.33351	0.66649	0.00067	330.000	7.883	376.48	0.125
0.33351	0.66649	0.00067	320.001	2.505	326.33	0.202
0.33351	0.66649	0.00067	325.008	4.201	336.07	0.178
0.33351	0.66649	0.00067	330.000	5.910	345.16	0.159
0.33351	0.66649	0.00067	330.000	5.932	346.00	0.158
0.33351	0.66649	0.00067	335.004	7.640	354.50	0.142
0.33351	0.66649	0.00067	325.006	2.664	303.74	0.240
0.33351	0.66649	0.00067	325.006	2.663	303.60	0.240
0.33351	0.66649	0.00067	329.998	4.248	314.22	0.208
0.33351	0.66649	0.00067	335.004	5.836	323.61	0.184
0.33351	0.66649	0.00067	329.997	2.987	284.75	0.279
0.33351	0.66649	0.00067	335.003	4.461	295.33	0.239
0.33351	0.66649	0.00067	340.008	5.942	304.74	0.209
0.33351	0.66649	0.00067	345.012	7.446	314.03	0.184
0.66643	0.33357	0.00034	229.999	0.471	687.99	0.046
0.66643	0.33357	0.00034	235.010	1.062	668.75	0.047
0.66643	0.33357	0.00034	240.003	1.077	645.73	0.049
0.66643	0.33357	0.00034	245.002	1.089	622.55	0.052
0.66643	0.33357	0.00034	250.004	1.120	599.62	0.055
0.66643	0.33357	0.00034	254.994	3.686	598.44	0.054
0.66643	0.33357	0.00034	259.986	7.231	605.38	0.052
0.66643	0.33357	0.00034	265.002	10.792	612.28	0.049
0.66643	0.33357	0.00034	269.992	14.364	619.27	0.048
0.66643	0.33357	0.00034	274.995	17.942	626.20	0.046
0.66643	0.33357	0.00034	279.999	21.515	633.02	0.044
0.66643	0.33357	0.00034	254.991	3.664	598.25	0.054
0.66643	0.33357	0.00034	254.991	1.737	582.05	0.058
0.66643	0.33357	0.00034	259.985	5.206	589.26	0.055
0.66643	0.33357	0.00034	269.991	12.115	603.11	0.050

Table 3 (continued)

x_1/mole frac	x_2/mole frac	$u_c(x_1)$/mole frac	T/K	p/MPa	w/m•s^{-1}	$U_c(w)$/ %
0.66643	0.33357	0.00034	259.984	1.506	557.12	0.062
0.66643	0.33357	0.00034	259.984	1.440	556.52	0.063
0.66643	0.33357	0.00034	269.990	7.924	570.42	0.056
0.66643	0.33357	0.00034	274.995	11.247	577.89	0.053
0.66643	0.33357	0.00034	269.991	4.788	543.12	0.063
0.66643	0.33357	0.00034	274.995	7.953	550.80	0.059
0.66643	0.33357	0.00034	279.999	11.132	558.41	0.056
0.66643	0.33357	0.00034	269.990	1.601	511.98	0.073
0.66643	0.33357	0.00034	274.994	4.576	519.80	0.068
0.66643	0.33357	0.00034	279.999	7.586	527.73	0.064
0.66643	0.33357	0.00034	285.001	10.594	535.45	0.060
0.66643	0.33357	0.00034	274.993	1.601	488.69	0.080
0.66643	0.33357	0.00034	279.998	4.428	496.85	0.075
0.66643	0.33357	0.00034	285.001	7.269	504.89	0.069
0.66643	0.33357	0.00034	290.002	10.119	512.75	0.065
0.66643	0.33357	0.00034	279.997	1.521	464.28	0.089
0.66643	0.33357	0.00034	284.999	4.185	472.69	0.082
0.66643	0.33357	0.00034	290.002	6.863	480.91	0.076
0.66643	0.33357	0.00034	294.998	9.551	488.94	0.071
0.66643	0.33357	0.00034	284.998	1.626	441.78	0.099
0.66643	0.33357	0.00034	290.001	4.149	450.52	0.091
0.66643	0.33357	0.00034	294.997	6.686	459.01	0.084
0.66643	0.33357	0.00034	299.998	9.233	467.24	0.078
0.66643	0.33357	0.00034	290.000	1.510	416.01	0.114
0.66643	0.33357	0.00034	294.995	3.867	425.01	0.103
0.66643	0.33357	0.00034	299.999	6.240	433.69	0.095
0.66643	0.33357	0.00034	304.996	8.625	442.10	0.087
0.66643	0.33357	0.00034	294.995	1.476	390.66	0.131
0.66643	0.33357	0.00034	299.997	3.687	400.09	0.118
0.66643	0.33357	0.00034	304.995	5.916	409.15	0.107
0.66643	0.33357	0.00034	309.999	8.157	417.85	0.098
0.66643	0.33357	0.00034	299.997	1.466	364.80	0.154
0.66643	0.33357	0.00034	304.996	3.547	374.94	0.137
0.66643	0.33357	0.00034	309.999	5.634	384.42	0.123
0.66643	0.33357	0.00034	314.993	7.728	393.41	0.112
0.66643	0.33357	0.00034	320.003	9.825	401.91	0.102
0.66643	0.33357	0.00034	304.993	1.937	347.12	0.171
0.66643	0.33357	0.00034	309.997	3.889	357.22	0.152
0.66643	0.33357	0.00034	314.989	5.848	366.71	0.136
0.66643	0.33357	0.00034	320.003	7.793	375.31	0.123
0.66643	0.33357	0.00034	325.008	9.761	383.72	0.112
0.66643	0.33357	0.00034	309.995	1.979	321.21	0.207

Table 3 (continued)

x_1/mole frac	x_2/mole frac	$u_c(x_1)$/mole frac	T/K	p/MPa	w/m•s^{-1}	$U_c(w)$/ %
0.66643	0.33357	0.00034	314.992	3.779	331.71	0.180
0.66643	0.33357	0.00034	320.003	5.598	341.52	0.160
0.66643	0.33357	0.00034	325.007	7.421	350.69	0.143
0.66643	0.33357	0.00034	314.991	2.245	299.27	0.245
0.66643	0.33357	0.00034	320.003	3.919	310.10	0.211
0.66643	0.33357	0.00034	325.008	5.605	319.71	0.184
0.66643	0.33357	0.00034	330.001	7.308	329.48	0.163

Compositions listed (x_1, x_2) and composition standard uncertainty ($u_c(x_1)$) are mole fractions. The standard uncertainties for temperature (T) and pressure (p) are $u_c(T)=0.004$ and $u_c(p)=0.014$ MPa, respectively. Speed of sound values listed (w) is averaged from up to twelve measurements at each state point. Relative combined expanded speed of sound uncertainties, $U_c(w)$, are determined with a coverage factor $k=2$ and include effects of composition, temperature, pressure, time delay between echo arrivals, and path length calibration as described in detail elsewhere [3, 4, 14]. Lines in the table separate the pseudo-isochores

the averaged speed of sound measurements for the R-125/1234yf, R-1234yf/152a, and R-1234ze(E)/227ea mixtures, respectively. Data listing up to twelve unaveraged speed of sound measurements and their associated uncertaities can be found in the supplementary information, and these data are also deposited at nist.data.gov (https://doi.org/10.18434/mds2-2642).

3.2 Comparison to REFPROP Mixture Models

Figure 2a to f are deviation graphs comparing the averaged speed of sound data listed in Tables 3, 4 and 5 to the current REFPROP [6] mixture models. Dashed lines in each figure are smoothed curves of the relative combined expanded speed of sound uncertainty of each measurement, which was described previously [3, 4]; these increase as the magnitude of the speed of sound decreases, and as the system approaches the blend's mixture critical point. The average absolute deviation, Δ_{AAD}, used to characterize the overall performance of each mixture model, is defined by

$$\Delta_{AAD} = 100 \cdot \frac{1}{N} \sum_{i=0}^{N} \left| \frac{w_{i,exp} - w_{i,calc}}{w_{i,exp}} \right|, \quad (1)$$

where $w_{i,exp}$ is an experimental speed of sound value, $w_{i,calc}$ is a calculated speed of sound value, and N is the number of data points evaluated. Additional statistical measures used to assess the present mixture models are the bias, Δ_{bias}, given by Eq. 2, and the maximum deviation, Δ_{max}, given by Eq. 3. Table 6 lists Δ_{AAD}, Δ_{bias}, and Δ_{max} for each mixture studied.

$$\Delta_{bias} = 100 \cdot \frac{1}{N} \sum_{i=0}^{N} \frac{w_{i,exp} - w_{i,calc}}{w_{i,exp}} \quad (2)$$

Table 4 Experimental speed of sound data for the R-1234yf/152a mixtures

x_1/mole frac	x_2/mole frac	$u_c(x_1)$/mole frac	T/K	p/MPa	w/m•s^{-1}	$U_c(w)$/ %
0.33342	0.66658	0.00070	229.998	0.258	874.02	0.039
0.33342	0.66658	0.00070	235.012	0.616	852.44	0.039
0.33342	0.66658	0.00070	240.002	0.620	828.74	0.040
0.33342	0.66658	0.00070	245.003	0.629	805.02	0.041
0.33342	0.66658	0.00070	250.005	0.639	781.39	0.043
0.33342	0.66658	0.00070	254.994	0.648	757.80	0.044
0.33342	0.66658	0.00070	259.987	0.663	734.27	0.046
0.33342	0.66658	0.00070	269.991	3.305	709.64	0.048
0.33342	0.66658	0.00070	269.991	3.290	709.46	0.048
0.33342	0.66658	0.00070	274.995	6.843	716.19	0.047
0.33342	0.66658	0.00070	279.999	10.500	723.65	0.045
0.33342	0.66658	0.00070	285.000	14.099	730.67	0.044
0.33342	0.66658	0.00070	269.990	1.083	690.61	0.050
0.33342	0.66658	0.00070	274.993	4.553	697.56	0.049
0.33342	0.66658	0.00070	279.998	8.034	704.54	0.047
0.33342	0.66658	0.00070	285.000	11.524	711.55	0.046
0.33342	0.66658	0.00070	274.992	1.087	667.01	0.053
0.33342	0.66658	0.00070	279.997	4.427	674.27	0.051
0.33342	0.66658	0.00070	284.999	7.776	681.55	0.050
0.33342	0.66658	0.00070	290.002	11.132	688.79	0.048
0.33342	0.66658	0.00070	279.997	1.131	643.60	0.057
0.33342	0.66658	0.00070	284.999	4.339	651.21	0.054
0.33342	0.66658	0.00070	290.002	7.563	658.80	0.052
0.33342	0.66658	0.00070	294.998	10.784	666.26	0.050
0.33342	0.66658	0.00070	284.998	1.054	618.93	0.061
0.33342	0.66658	0.00070	290.001	4.120	626.79	0.058
0.33342	0.66658	0.00070	294.998	7.188	634.51	0.056
0.33342	0.66658	0.00070	299.998	10.264	642.13	0.053
0.33342	0.66658	0.00070	289.999	1.178	596.19	0.065
0.33342	0.66658	0.00070	294.996	4.113	604.32	0.062
0.33342	0.66658	0.00070	299.998	7.056	612.29	0.059
0.33342	0.66658	0.00070	304.996	9.987	619.96	0.057
0.33342	0.66658	0.00070	294.995	1.011	570.00	0.072
0.33342	0.66658	0.00070	299.997	3.806	578.42	0.068
0.33342	0.66658	0.00070	304.997	6.615	586.74	0.064
0.33342	0.66658	0.00070	309.999	9.429	594.83	0.061
0.33342	0.66658	0.00070	299.996	1.209	547.74	0.078
0.33342	0.66658	0.00070	304.996	3.847	556.10	0.073
0.33342	0.66658	0.00070	309.998	6.521	564.52	0.069
0.33342	0.66658	0.00070	314.993	9.198	572.72	0.065
0.33342	0.66658	0.00070	304.994	1.263	523.56	0.086
0.33342	0.66658	0.00070	309.998	3.817	532.72	0.080

Table 4 (continued)

x_1/mole frac	x_2/mole frac	$u_c(x_1)$/mole frac	T/K	p/MPa	w/m•s^{-1}	$U_c(w)$/ %
0.33342	0.66658	0.00070	314.994	6.372	541.49	0.075
0.33342	0.66658	0.00070	320.003	8.940	550.04	0.070
0.33342	0.66658	0.00070	309.997	1.356	499.49	0.096
0.33342	0.66658	0.00070	314.993	3.833	509.65	0.088
0.33342	0.66658	0.00070	320.003	6.276	518.79	0.082
0.33342	0.66658	0.00070	325.009	8.703	527.34	0.076
0.33342	0.66658	0.00070	314.991	1.651	478.24	0.106
0.33342	0.66658	0.00070	320.002	3.967	487.98	0.097
0.33342	0.66658	0.00070	325.008	6.266	497.03	0.089
0.33342	0.66658	0.00070	329.999	8.556	505.58	0.083
0.33342	0.66658	0.00070	320.003	1.697	452.76	0.120
0.33342	0.66658	0.00070	325.007	3.876	462.80	0.109
0.33342	0.66658	0.00070	329.999	6.042	472.10	0.100
0.33342	0.66658	0.00070	335.004	8.198	480.75	0.093
0.33342	0.66658	0.00070	325.007	1.969	430.73	0.135
0.33342	0.66658	0.00070	329.999	4.027	441.05	0.122
0.33342	0.66658	0.00070	335.003	6.081	450.54	0.111
0.33342	0.66658	0.00070	340.008	8.146	459.65	0.102
0.33342	0.66658	0.00070	329.997	2.042	404.69	0.158
0.33342	0.66658	0.00070	335.002	3.952	415.02	0.141
0.33342	0.66658	0.00070	340.006	5.886	424.93	0.127
0.33342	0.66658	0.00070	345.012	7.830	434.39	0.116
0.33342	0.66658	0.00070	335.000	2.091	377.02	0.189
0.33342	0.66658	0.00070	340.007	3.904	388.49	0.166
0.33342	0.66658	0.00070	345.013	5.729	399.14	0.147
0.33342	0.66658	0.00070	340.007	2.413	354.81	0.220
0.33342	0.66658	0.00070	345.013	4.107	366.51	0.190
0.66526	0.33474	0.00055	229.996	0.135	800.24	0.043
0.66526	0.33474	0.00055	235.011	0.631	780.26	0.041
0.66526	0.33474	0.00055	240.002	0.648	757.43	0.042
0.66526	0.33474	0.00055	245.002	0.654	734.42	0.044
0.66526	0.33474	0.00055	250.004	0.671	711.50	0.046
0.66526	0.33474	0.00055	254.994	0.670	688.76	0.048
0.66526	0.33474	0.00055	259.987	3.819	691.33	0.047
0.66526	0.33474	0.00055	259.985	0.833	667.24	0.050
0.66526	0.33474	0.00055	274.995	11.612	688.91	0.046
0.66526	0.33474	0.00055	269.990	3.405	644.51	0.052
0.66526	0.33474	0.00055	274.995	6.857	652.38	0.050
0.66526	0.33474	0.00055	279.999	10.264	659.74	0.049
0.66526	0.33474	0.00055	269.991	1.171	624.61	0.056
0.66526	0.33474	0.00055	274.994	4.478	632.30	0.054
0.66526	0.33474	0.00055	279.999	7.793	639.91	0.051

Table 4 (continued)

x_1/mole frac	x_2/mole frac	$u_c(x_1)$/mole frac	T/K	p/MPa	w/m•s^{-1}	$U_c(w)$/ %
0.66526	0.33474	0.00055	285.000	11.120	647.51	0.050
0.66526	0.33474	0.00055	274.992	1.269	602.80	0.059
0.66526	0.33474	0.00055	279.999	4.441	610.74	0.057
0.66526	0.33474	0.00055	285.000	7.628	618.62	0.054
0.66526	0.33474	0.00055	290.002	10.799	626.23	0.052
0.66526	0.33474	0.00055	279.997	1.047	577.69	0.064
0.66526	0.33474	0.00055	284.999	4.067	585.91	0.061
0.66526	0.33474	0.00055	290.002	7.093	593.95	0.058
0.66526	0.33474	0.00055	294.998	10.116	601.80	0.055
0.66526	0.33474	0.00055	284.998	1.082	554.99	0.070
0.66526	0.33474	0.00055	290.001	3.963	563.43	0.066
0.66526	0.33474	0.00055	294.998	6.851	571.70	0.062
0.66526	0.33474	0.00055	299.999	9.742	579.75	0.059
0.66526	0.33474	0.00055	290.000	1.026	531.01	0.076
0.66526	0.33474	0.00055	294.997	3.769	539.79	0.071
0.66526	0.33474	0.00055	299.999	6.519	548.29	0.067
0.66526	0.33474	0.00055	304.997	9.267	556.50	0.063
0.66526	0.33474	0.00055	294.995	1.115	508.59	0.083
0.66526	0.33474	0.00055	299.996	3.725	517.58	0.078
0.66526	0.33474	0.00055	304.997	6.342	526.29	0.072
0.66526	0.33474	0.00055	309.999	8.958	534.65	0.068
0.66526	0.33474	0.00055	299.995	1.325	487.63	0.091
0.66526	0.33474	0.00055	304.996	3.806	496.79	0.084
0.66526	0.33474	0.00055	309.998	6.298	505.65	0.078
0.66526	0.33474	0.00055	314.994	8.789	514.15	0.073
0.66526	0.33474	0.00055	304.994	1.369	464.23	0.102
0.66526	0.33474	0.00055	309.998	3.725	473.73	0.093
0.66526	0.33474	0.00055	314.993	6.084	482.82	0.086
0.66526	0.33474	0.00055	320.004	8.452	491.54	0.080
0.66526	0.33474	0.00055	309.996	1.617	443.53	0.113
0.66526	0.33474	0.00055	314.993	3.849	453.25	0.103
0.66526	0.33474	0.00055	320.003	6.090	462.47	0.094
0.66526	0.33474	0.00055	325.007	8.351	471.47	0.087
0.66526	0.33474	0.00055	314.991	1.659	419.51	0.128
0.66526	0.33474	0.00055	320.002	3.757	429.41	0.116
0.66526	0.33474	0.00055	325.008	5.845	438.60	0.106
0.66526	0.33474	0.00055	329.999	7.970	447.76	0.097
0.66526	0.33474	0.00055	320.000	1.690	394.59	0.149
0.66526	0.33474	0.00055	325.007	3.656	404.85	0.133
0.66526	0.33474	0.00055	329.999	5.625	414.48	0.121
0.66526	0.33474	0.00055	335.003	7.587	423.38	0.110
0.66526	0.33474	0.00055	325.006	2.087	376.15	0.166

Table 4 (continued)

x_1/mole frac	x_2/mole frac	$u_c(x_1)$/mole frac	T/K	p/MPa	w/m•s^{-1}	$U_c(w)$/ %
0.66526	0.33474	0.00055	329.998	3.941	386.52	0.148
0.66526	0.33474	0.00055	335.003	5.793	396.02	0.133
0.66526	0.33474	0.00055	340.008	7.662	405.17	0.121
0.66526	0.33474	0.00055	329.996	1.939	346.06	0.206
0.66526	0.33474	0.00055	335.003	3.635	356.72	0.181
0.66526	0.33474	0.00055	340.007	5.349	366.76	0.160
0.66526	0.33474	0.00055	345.013	7.070	376.19	0.144
0.66526	0.33474	0.00055	335.001	2.211	324.32	0.241
0.66526	0.33474	0.00055	340.007	3.804	335.47	0.209
0.66526	0.33474	0.00055	345.013	5.407	345.72	0.183
0.66526	0.33474	0.00055	340.007	2.757	309.92	0.266
0.66526	0.33474	0.00055	345.013	4.263	320.63	0.229

Compositions listed (x_1, x_2) and composition standard uncertainty ($u_c(x_1)$) are mole fractions. The standard uncertainties for temperature (T) and pressure (p) are $u_c(T)=0.004$ and $u_c(p)=0.014$ MPa, respectively. Speed of sound values listed (w) are averaged from up to twelve measurements at each state point. Relative combined expanded speed of sound uncertainties, $U_c(w)$, are determined with a coverage factor $k=2$, and include effects of composition, temperature, pressure, time delay between echo arrivals, and path length calibration as described in detail elsewhere [3, 4, 14]. Lines in the table separate the pseudo-isochores

$$\Delta_{\max} = \max\left(100 \cdot \left| \frac{w_{i,\exp} - w_{i,\mathrm{calc}}}{w_{i,\exp}} \right| \right) \tag{3}$$

The Δ_{AAD} values vary from 0.10 % to 0.27 % for the R-125/1234yf and R-1234yf/152a mixtures. However, the Δ_{AAD} values for the R-1234ze(E)/227ea mixtures are significantly greater, ranging from 0.62 % to 0.94 %. The maximum deviation ranges from 0.18 % to 0.68 % for the R-125/1234yf and R-1234yf/152a mixtures and as high as 3.57 % for the R-1234ze(E)/227ea mixtures. Figure 2a and b shows that the current REFPROP[6] models calculate speed of sound values that are slightly higher (Δ_{bias} of −0.12 % to −0.27 %) than the reported experimental data for R-125/1234yf mixtures and as shown in Fig. 2c and b slightly lower speed of sound values (Δ_{bias} of 0.08 %) for the R-1234yf/152a mixtures. This shows that the current REFPROP mixture models for R-125/1234yf and R-1234yf/152a mixtures only require slight adjustments to accurately represent the blends respective speed of sounds. However, as shown in Fig. 2e and f, the current REFPROP speed of sound calculations for R-1234ze(E)/227ea are substantially higher (Δ_{bias} of −0.62 % to −0.94 %) than the experimental values reported here. The greater deviations seen with the R-1234ze(E)/227ea mixtures are not unexpected since (1) as shown by McLinden and Perkins [14] and Bell [5] the current EOS for pure R-1234ze(E) requires further adjustments to accurately match experimental speed of sound data, and (2) no binary interaction parameters

Table 5 Experimental speed of sound data for the R-1234ze(E)/227ea mixtures

x_1/mole frac	x_2/mole frac	$u_c(x_1)$/mole frac	T/K	p/MPa	w/m•s^{-1}	$U_c(w)$/ %
0.33265	0.66737	0.00023	230.010	0.370	736.85	0.040
0.33265	0.66737	0.00023	235.012	0.457	715.38	0.041
0.33265	0.66737	0.00023	240.001	0.462	693.46	0.043
0.33265	0.66737	0.00023	245.003	0.469	671.70	0.044
0.33265	0.66737	0.00023	250.004	0.465	650.04	0.046
0.33265	0.66737	0.00023	254.995	0.458	628.53	0.048
0.33265	0.66737	0.00023	259.987	0.471	607.24	0.051
0.33265	0.66737	0.00023	269.992	3.351	588.48	0.052
0.33265	0.66737	0.00023	274.995	6.712	594.84	0.050
0.33265	0.66737	0.00023	279.999	10.082	601.22	0.049
0.33265	0.66737	0.00023	285.000	13.433	607.45	0.047
0.33265	0.66737	0.00023	290.002	16.668	612.91	0.046
0.33265	0.66737	0.00023	294.997	19.952	618.72	0.045
0.33265	0.66737	0.00023	299.998	23.210	624.35	0.044
0.33265	0.66737	0.00023	304.997	26.420	629.72	0.043
0.33265	0.66737	0.00023	309.999	29.616	635.01	0.042
0.33265	0.66737	0.00023	314.994	32.783	640.19	0.041
0.33265	0.66737	0.00023	320.005	35.925	645.23	0.041
0.33265	0.66737	0.00023	325.010	39.103	650.48	0.040
0.33265	0.66737	0.00023	330.000	42.303	655.89	0.039
0.33265	0.66737	0.00023	335.003	45.456	661.01	0.039
0.33265	0.66737	0.00023	340.008	48.628	666.24	0.039
0.33265	0.66737	0.00023	274.991	3.582	570.38	0.055
0.33265	0.66737	0.00023	279.996	6.857	577.23	0.052
0.33265	0.66737	0.00023	284.997	10.129	583.99	0.050
0.33265	0.66737	0.00023	289.999	13.388	590.58	0.049
0.33265	0.66737	0.00023	294.995	16.634	597.03	0.047
0.33265	0.66737	0.00023	299.997	19.861	603.31	0.046
0.33265	0.66737	0.00023	304.996	23.080	609.49	0.045
0.33265	0.66737	0.00023	309.998	26.280	615.51	0.044
0.33265	0.66737	0.00023	314.994	29.441	621.29	0.043
0.33265	0.66737	0.00023	320.002	32.633	627.19	0.042
0.33265	0.66737	0.00023	325.008	35.791	632.89	0.041
0.33265	0.66737	0.00023	330.000	38.917	638.43	0.041
0.33265	0.66737	0.00023	335.003	41.992	643.65	0.040
0.33265	0.66737	0.00023	340.007	45.084	648.96	0.039
0.33265	0.66737	0.00023	345.013	48.160	654.19	0.039
0.33265	0.66737	0.00023	269.987	0.427	564.48	0.057
0.33265	0.66737	0.00023	274.990	0.887	547.36	0.060
0.33265	0.66737	0.00023	279.995	4.051	554.51	0.057
0.33265	0.66737	0.00023	284.997	7.216	561.58	0.054
0.33265	0.66737	0.00023	289.999	10.386	568.56	0.052

Table 5 (continued)

x_1/mole frac	x_2/mole frac	$u_c(x_1)$/mole frac	T/K	p/MPa	w/m•s^{-1}	$U_c(w)$/ %
0.33265	0.66737	0.00023	294.995	13.539	575.34	0.050
0.33265	0.66737	0.00023	299.997	16.693	582.02	0.049
0.33265	0.66737	0.00023	304.993	19.799	588.33	0.047
0.33265	0.66737	0.00023	309.998	22.889	594.43	0.046
0.33265	0.66737	0.00023	314.992	25.989	600.59	0.045
0.33265	0.66737	0.00023	320.002	29.081	606.63	0.044
0.33265	0.66737	0.00023	325.008	32.153	612.51	0.043
0.33265	0.66737	0.00023	329.999	35.201	618.26	0.042
0.33265	0.66737	0.00023	335.001	38.214	623.77	0.041
0.33265	0.66737	0.00023	340.008	41.230	629.27	0.041
0.33265	0.66737	0.00023	345.013	44.228	634.66	0.040
0.33265	0.66737	0.00023	279.993	0.975	527.12	0.064
0.33265	0.66737	0.00023	284.995	3.998	534.47	0.060
0.33265	0.66737	0.00023	289.998	7.035	541.78	0.057
0.33265	0.66737	0.00023	294.994	10.056	548.85	0.055
0.33265	0.66737	0.00023	299.996	13.128	556.12	0.053
0.33265	0.66737	0.00023	304.995	16.175	563.14	0.051
0.33265	0.66737	0.00023	309.997	19.195	569.83	0.049
0.33265	0.66737	0.00023	314.993	22.200	576.33	0.048
0.33265	0.66737	0.00023	320.003	25.195	582.67	0.046
0.33265	0.66737	0.00023	325.007	28.171	588.82	0.045
0.33265	0.66737	0.00023	329.999	31.120	594.79	0.044
0.33265	0.66737	0.00023	335.002	34.026	600.43	0.043
0.33265	0.66737	0.00023	340.008	36.936	606.06	0.043
0.33265	0.66737	0.00023	345.013	39.848	611.67	0.042
0.33265	0.66737	0.00023	284.994	0.925	505.60	0.069
0.33265	0.66737	0.00023	289.997	3.800	513.12	0.065
0.33265	0.66737	0.00023	294.993	6.684	520.55	0.061
0.33265	0.66737	0.00023	299.994	9.524	527.43	0.059
0.33265	0.66737	0.00023	304.994	12.394	534.42	0.056
0.33265	0.66737	0.00023	309.997	15.271	541.34	0.054
0.33265	0.66737	0.00023	314.992	18.133	548.04	0.052
0.33265	0.66737	0.00023	320.002	20.996	554.62	0.050
0.33265	0.66737	0.00023	325.008	23.843	561.00	0.049
0.33265	0.66737	0.00023	329.999	26.667	567.19	0.047
0.33265	0.66737	0.00023	335.005	29.464	573.11	0.046
0.33265	0.66737	0.00023	340.007	32.254	578.94	0.045
0.33265	0.66737	0.00023	345.013	35.038	584.69	0.044
0.33265	0.66737	0.00023	289.996	0.986	485.10	0.074
0.33265	0.66737	0.00023	294.993	3.735	492.94	0.070
0.33265	0.66737	0.00023	299.993	6.490	500.58	0.066
0.33265	0.66737	0.00023	304.994	9.299	508.47	0.062

Table 5 (continued)

x_1/mole frac	x_2/mole frac	$u_c(x_1)$/mole frac	T/K	p/MPa	w/m•s^{-1}	$U_c(w)$/ %
0.33265	0.66737	0.00023	309.996	12.075	515.88	0.059
0.33265	0.66737	0.00023	314.992	14.830	522.96	0.057
0.33265	0.66737	0.00023	320.002	17.582	529.82	0.055
0.33265	0.66737	0.00023	325.007	20.318	536.45	0.053
0.33265	0.66737	0.00023	329.999	23.036	542.79	0.051
0.33265	0.66737	0.00023	335.001	25.715	548.91	0.049
0.33265	0.66737	0.00023	340.008	28.405	554.95	0.048
0.33265	0.66737	0.00023	345.012	31.087	560.88	0.047
0.33265	0.66737	0.00023	294.991	1.091	465.10	0.081
0.33265	0.66737	0.00023	299.993	3.721	473.25	0.075
0.33265	0.66737	0.00023	304.992	6.347	481.07	0.071
0.33265	0.66737	0.00023	309.995	8.983	488.72	0.067
0.33265	0.66737	0.00023	314.991	11.611	496.09	0.063
0.33265	0.66737	0.00023	320.001	14.242	503.27	0.060
0.33265	0.66737	0.00023	325.006	16.854	510.15	0.058
0.33265	0.66737	0.00023	330.000	19.503	517.17	0.056
0.33265	0.66737	0.00023	335.002	22.092	523.63	0.053
0.33265	0.66737	0.00023	340.006	24.669	529.88	0.052
0.33265	0.66737	0.00023	345.012	27.238	535.98	0.050
0.33265	0.66737	0.00023	299.992	1.009	442.88	0.089
0.33265	0.66737	0.00023	304.993	3.494	451.20	0.083
0.33265	0.66737	0.00023	309.995	5.961	459.03	0.077
0.33265	0.66737	0.00023	314.990	8.434	466.60	0.073
0.33265	0.66737	0.00023	320.000	10.921	474.06	0.069
0.33265	0.66737	0.00023	325.007	13.407	481.32	0.065
0.33265	0.66737	0.00023	329.997	15.871	488.25	0.062
0.33265	0.66737	0.00023	335.003	18.295	494.68	0.060
0.33265	0.66737	0.00023	340.007	20.733	501.07	0.057
0.33265	0.66737	0.00023	345.012	23.173	507.39	0.055
0.33265	0.66737	0.00023	304.990	1.109	422.59	0.098
0.33265	0.66737	0.00023	309.994	3.483	431.35	0.091
0.33265	0.66737	0.00023	314.990	5.860	439.72	0.084
0.33265	0.66737	0.00023	320.000	8.241	447.73	0.078
0.33265	0.66737	0.00023	325.007	10.617	455.41	0.074
0.33265	0.66737	0.00023	329.996	12.978	462.75	0.070
0.33265	0.66737	0.00023	335.001	15.291	469.45	0.066
0.33265	0.66737	0.00023	340.007	17.608	475.99	0.063
0.33265	0.66737	0.00023	345.012	19.938	482.52	0.061
0.33265	0.66737	0.00023	309.994	1.305	403.55	0.108
0.33265	0.66737	0.00023	314.991	3.546	412.37	0.099
0.33265	0.66737	0.00023	320.000	5.801	420.82	0.092
0.33265	0.66737	0.00023	325.008	8.053	428.88	0.085

Table 5 (continued)

x_1/mole frac	x_2/mole frac	$u_c(x_1)$/mole frac	T/K	p/MPa	w/m•s^{-1}	$U_c(w)$/ %
0.33265	0.66737	0.00023	329.997	10.294	436.56	0.080
0.33265	0.66737	0.00023	335.002	12.528	443.85	0.075
0.33265	0.66737	0.00023	340.006	14.762	450.93	0.071
0.33265	0.66737	0.00023	345.012	16.994	457.79	0.068
0.33265	0.66737	0.00023	314.988	1.411	383.28	0.121
0.33265	0.66737	0.00023	319.999	3.535	392.36	0.110
0.33265	0.66737	0.00023	325.006	5.662	400.95	0.101
0.33265	0.66737	0.00023	329.998	7.782	409.07	0.094
0.33265	0.66737	0.00023	335.001	9.886	416.62	0.087
0.33265	0.66737	0.00023	340.007	12.002	424.04	0.082
0.33265	0.66737	0.00023	345.013	14.117	431.21	0.077
0.33265	0.66737	0.00023	319.999	1.467	361.90	0.138
0.33265	0.66737	0.00023	325.005	3.458	371.11	0.125
0.33265	0.66737	0.00023	329.997	5.448	379.87	0.114
0.33265	0.66737	0.00023	335.004	7.431	387.97	0.105
0.33265	0.66737	0.00023	340.005	9.423	395.78	0.097
0.33265	0.66737	0.00023	345.012	11.417	403.31	0.090
0.33265	0.66737	0.00023	325.005	1.545	340.60	0.159
0.33265	0.66737	0.00023	329.996	3.405	350.07	0.143
0.33265	0.66737	0.00023	335.002	5.258	358.70	0.129
0.33265	0.66737	0.00023	340.007	7.124	367.01	0.118
0.33265	0.66737	0.00023	345.012	8.997	374.99	0.108
0.33265	0.66737	0.00023	329.997	1.695	320.21	0.184
0.33265	0.66737	0.00023	335.001	3.431	329.77	0.163
0.33265	0.66737	0.00023	340.006	5.178	338.76	0.146
0.33265	0.66737	0.00023	345.012	6.933	347.28	0.133
0.33265	0.66737	0.00023	335.000	1.674	295.57	0.224
0.33265	0.66737	0.00023	340.006	3.281	305.80	0.196
0.33265	0.66737	0.00023	345.013	4.898	315.09	0.173
0.33265	0.66737	0.00023	340.006	1.985	278.05	0.258
0.33265	0.66737	0.00023	345.012	3.488	288.00	0.224
0.33265	0.66737	0.00023	345.012	2.126	255.72	0.317
0.66803	0.33197	0.00023	230.003	0.053	779.72	0.041
0.66803	0.33197	0.00023	235.014	0.063	757.30	0.041
0.66803	0.33197	0.00023	239.996	0.074	734.91	0.041
0.66803	0.33197	0.00023	245.001	0.088	712.53	0.042
0.66803	0.33197	0.00023	250.004	0.107	690.31	0.044
0.66803	0.33197	0.00023	254.994	0.129	668.28	0.047
0.66803	0.33197	0.00023	259.987	0.152	646.36	0.048
0.66803	0.33197	0.00023	269.988	0.213	602.62	0.053
0.66803	0.33197	0.00023	274.996	0.253	580.89	0.057
0.66803	0.33197	0.00023	279.999	0.298	559.19	0.060

Table 5 (continued)

x_1/mole frac	x_2/mole frac	$u_c(x_1)$/mole frac	T/K	p/MPa	w/m•s^{-1}	$U_c(w)$/ %
0.66803	0.33197	0.00023	285.001	0.347	537.52	0.065
0.66803	0.33197	0.00023	290.003	0.406	515.85	0.070
0.66803	0.33197	0.00023	235.009	0.447	759.58	0.044
0.66803	0.33197	0.00023	240.003	0.452	737.64	0.043
0.66803	0.33197	0.00023	240.003	0.455	737.19	0.042
0.66803	0.33197	0.00023	245.005	0.462	715.20	0.042
0.66803	0.33197	0.00023	250.002	0.465	693.13	0.044
0.66803	0.33197	0.00023	254.987	0.469	670.84	0.047
0.66803	0.33197	0.00023	259.986	0.475	648.96	0.048
0.66803	0.33197	0.00023	269.990	1.033	609.66	0.052
0.66803	0.33197	0.00023	274.995	4.491	616.43	0.050
0.66803	0.33197	0.00023	280.000	8.049	623.90	0.048
0.66803	0.33197	0.00023	285.001	11.526	630.69	0.047
0.66803	0.33197	0.00023	290.003	14.982	637.28	0.046
0.66803	0.33197	0.00023	294.998	18.419	643.73	0.044
0.66803	0.33197	0.00023	299.999	21.844	650.05	0.043
0.66803	0.33197	0.00023	304.997	25.231	656.12	0.042
0.66803	0.33197	0.00023	309.999	28.622	662.19	0.042
0.66803	0.33197	0.00023	314.995	31.989	668.12	0.041
0.66803	0.33197	0.00023	320.004	35.312	673.76	0.040
0.66803	0.33197	0.00023	320.005	35.204	673.17	0.040
0.66803	0.33197	0.00023	325.009	38.483	678.61	0.040
0.66803	0.33197	0.00023	330.000	41.708	683.81	0.039
0.66803	0.33197	0.00023	335.002	44.866	688.64	0.039
0.66803	0.33197	0.00023	340.007	48.022	693.49	0.038
0.66803	0.33197	0.00023	274.992	1.213	589.52	0.055
0.66803	0.33197	0.00023	279.997	4.543	596.58	0.053
0.66803	0.33197	0.00023	284.999	7.874	603.58	0.051
0.66803	0.33197	0.00023	290.001	11.198	610.44	0.049
0.66803	0.33197	0.00023	294.995	14.510	617.16	0.048
0.66803	0.33197	0.00023	299.999	17.813	623.75	0.046
0.66803	0.33197	0.00023	304.996	21.164	630.60	0.045
0.66803	0.33197	0.00023	309.999	24.461	637.03	0.044
0.66803	0.33197	0.00023	314.994	27.724	643.24	0.043
0.66803	0.33197	0.00023	320.002	30.973	649.28	0.042
0.66803	0.33197	0.00023	325.009	34.192	655.13	0.041
0.66803	0.33197	0.00023	330.000	37.386	660.86	0.041
0.66803	0.33197	0.00023	335.003	40.524	666.24	0.040
0.66803	0.33197	0.00023	340.008	43.670	671.65	0.039
0.66803	0.33197	0.00023	345.013	46.803	677.00	0.039
0.66803	0.33197	0.00023	279.994	1.084	566.73	0.059
0.66803	0.33197	0.00023	284.996	4.255	573.96	0.056

Table 5 (continued)

x_1/mole frac	x_2/mole frac	$u_c(x_1)$/mole frac	T/K	p/MPa	w/m•s^{-1}	$U_c(w)$/ %
0.66803	0.33197	0.00023	289.999	7.438	581.18	0.054
0.66803	0.33197	0.00023	294.993	10.579	587.99	0.052
0.66803	0.33197	0.00023	299.995	13.705	594.56	0.050
0.66803	0.33197	0.00023	304.995	16.862	601.31	0.048
0.66803	0.33197	0.00023	309.998	20.016	607.96	0.047
0.66803	0.33197	0.00023	314.992	23.151	614.44	0.046
0.66803	0.33197	0.00023	320.003	26.278	620.77	0.045
0.66803	0.33197	0.00023	325.008	29.384	626.92	0.044
0.66803	0.33197	0.00023	329.999	32.463	632.91	0.043
0.66803	0.33197	0.00023	335.003	35.506	638.62	0.042
0.66803	0.33197	0.00023	340.006	38.543	644.27	0.041
0.66803	0.33197	0.00023	345.012	41.571	649.86	0.040
0.66803	0.33197	0.00023	284.994	1.314	547.20	0.062
0.66803	0.33197	0.00023	289.997	4.365	554.74	0.059
0.66803	0.33197	0.00023	294.993	7.420	562.17	0.056
0.66803	0.33197	0.00023	299.995	10.466	569.36	0.054
0.66803	0.33197	0.00023	304.994	13.507	576.39	0.052
0.66803	0.33197	0.00023	309.998	16.549	583.31	0.050
0.66803	0.33197	0.00023	314.991	19.574	590.05	0.049
0.66803	0.33197	0.00023	320.003	22.645	596.98	0.047
0.66803	0.33197	0.00023	325.008	25.638	603.29	0.046
0.66803	0.33197	0.00023	329.999	28.613	609.46	0.045
0.66803	0.33197	0.00023	335.003	31.531	615.19	0.044
0.66803	0.33197	0.00023	340.007	34.458	620.96	0.043
0.66803	0.33197	0.00023	345.012	37.380	626.67	0.042
0.66803	0.33197	0.00023	289.995	1.137	523.75	0.068
0.66803	0.33197	0.00023	294.992	3.997	531.14	0.064
0.66803	0.33197	0.00023	299.994	6.895	538.71	0.061
0.66803	0.33197	0.00023	304.993	9.787	546.05	0.058
0.66803	0.33197	0.00023	309.995	12.667	553.14	0.056
0.66803	0.33197	0.00023	314.992	15.528	559.98	0.054
0.66803	0.33197	0.00023	320.001	18.364	566.48	0.052
0.66803	0.33197	0.00023	325.007	21.179	572.77	0.050
0.66803	0.33197	0.00023	329.999	23.976	578.90	0.049
0.66803	0.33197	0.00023	335.002	26.756	584.82	0.047
0.66803	0.33197	0.00023	340.007	29.549	590.79	0.046
0.66803	0.33197	0.00023	345.012	32.341	596.71	0.045
0.66803	0.33197	0.00023	294.991	1.279	503.42	0.073
0.66803	0.33197	0.00023	299.993	4.055	511.48	0.068
0.66803	0.33197	0.00023	304.993	6.835	519.32	0.065
0.66803	0.33197	0.00023	309.995	9.617	526.94	0.061
0.66803	0.33197	0.00023	314.989	12.347	533.99	0.059

Table 5 (continued)

x_1/mole frac	x_2/mole frac	$u_c(x_1)$/mole frac	T/K	p/MPa	w/m•s^{-1}	$U_c(w)$/ %
0.66803	0.33197	0.00023	320.002	15.098	540.97	0.056
0.66803	0.33197	0.00023	325.007	17.854	547.90	0.054
0.66803	0.33197	0.00023	329.998	20.587	554.59	0.052
0.66803	0.33197	0.00023	335.002	23.303	561.00	0.051
0.66803	0.33197	0.00023	340.007	26.013	567.28	0.049
0.66803	0.33197	0.00023	345.012	28.714	573.45	0.048
0.66803	0.33197	0.00023	299.992	1.292	481.62	0.079
0.66803	0.33197	0.00023	304.992	3.994	490.59	0.074
0.66803	0.33197	0.00023	309.995	6.699	499.19	0.069
0.66803	0.33197	0.00023	314.991	9.396	507.42	0.066
0.66803	0.33197	0.00023	320.002	12.108	515.43	0.062
0.66803	0.33197	0.00023	325.006	14.789	523.00	0.059
0.66803	0.33197	0.00023	329.998	17.455	530.26	0.057
0.66803	0.33197	0.00023	335.002	20.098	537.17	0.055
0.66803	0.33197	0.00023	340.008	22.742	543.94	0.053
0.66803	0.33197	0.00023	345.012	25.378	550.54	0.051
0.66803	0.33197	0.00023	304.991	1.176	458.03	0.088
0.66803	0.33197	0.00023	309.995	3.732	467.27	0.081
0.66803	0.33197	0.00023	314.989	6.283	476.05	0.076
0.66803	0.33197	0.00023	320.000	8.832	484.35	0.071
0.66803	0.33197	0.00023	325.006	11.370	492.28	0.068
0.66803	0.33197	0.00023	329.998	13.920	500.10	0.064
0.66803	0.33197	0.00023	335.003	16.403	507.12	0.061
0.66803	0.33197	0.00023	340.008	18.918	514.18	0.059
0.66803	0.33197	0.00023	345.013	21.422	521.04	0.056
0.66803	0.33197	0.00023	309.993	1.287	437.02	0.097
0.66803	0.33197	0.00023	314.990	3.694	446.31	0.089
0.66803	0.33197	0.00023	320.001	6.108	455.14	0.083
0.66803	0.33197	0.00023	325.006	8.485	463.18	0.078
0.66803	0.33197	0.00023	329.998	10.848	470.83	0.073
0.66803	0.33197	0.00023	335.001	13.187	478.01	0.070
0.66803	0.33197	0.00023	340.006	15.524	484.95	0.066
0.66803	0.33197	0.00023	345.012	17.878	491.88	0.063
0.66803	0.33197	0.00023	314.988	1.421	416.15	0.108
0.66803	0.33197	0.00023	319.999	3.707	425.71	0.099
0.66803	0.33197	0.00023	325.004	5.990	434.69	0.092
0.66803	0.33197	0.00023	329.997	8.262	443.16	0.085
0.66803	0.33197	0.00023	335.002	10.522	451.08	0.080
0.66803	0.33197	0.00023	340.008	12.787	458.77	0.075
0.66803	0.33197	0.00023	345.012	15.055	466.24	0.071
0.66803	0.33197	0.00023	319.999	1.571	395.33	0.121
0.66803	0.33197	0.00023	325.006	3.713	404.91	0.110

Table 5 (continued)

x_1/mole frac	x_2/mole frac	$u_c(x_1)$/mole frac	T/K	p/MPa	w/m•s^{-1}	$U_c(w)$/ %
0.66803	0.33197	0.00023	329.997	5.840	413.74	0.101
0.66803	0.33197	0.00023	335.001	7.947	421.83	0.094
0.66803	0.33197	0.00023	340.007	10.060	429.66	0.088
0.66803	0.33197	0.00023	345.013	12.157	437.02	0.083
0.66803	0.33197	0.00023	325.004	1.528	371.16	0.139
0.66803	0.33197	0.00023	329.996	3.533	381.13	0.126
0.66803	0.33197	0.00023	335.002	5.533	390.25	0.115
0.66803	0.33197	0.00023	340.007	7.545	399.01	0.106
0.66803	0.33197	0.00023	345.013	9.561	407.38	0.098
0.66803	0.33197	0.00023	329.997	1.761	351.24	0.158
0.66803	0.33197	0.00023	335.001	3.610	360.73	0.143
0.66803	0.33197	0.00023	340.007	5.462	369.61	0.130
0.66803	0.33197	0.00023	345.012	7.292	377.62	0.120
0.66803	0.33197	0.00023	335.000	1.723	325.61	0.191
0.66803	0.33197	0.00023	340.006	3.470	336.18	0.169
0.66803	0.33197	0.00023	345.012	5.221	345.86	0.151
0.66803	0.33197	0.00023	340.005	2.029	306.65	0.220
0.66803	0.33197	0.00023	345.012	3.661	317.29	0.193
0.66803	0.33197	0.00023	345.013	1.861	275.26	0.292

Compositions listed (x_1, x_2) and composition standard uncertainty ($u_c(x_1)$) are mole fractions. The standard uncertainties for temperature (T) and pressure (p) are $u_c(T) = 0.004$ and $u_c(p) = 0.014$ MPa, respectively. Speed of sound values listed (w) are averaged from up to twelve measurements at each state point. Relative combined expanded speed of sound uncertainties, $U_c(w)$, are determined with a coverage factor $k = 2$, and include effects of composition, temperature, pressure, time delay between echo arrivals, and path length calibration as described in detail elsewhere [3, 4, 14]. Lines in the table separate the pseudo-isochores

for the R-1234ze(E)/227ea system exist, and therefore, parameters for the chemically similar system R-1234yf/227ea [12] were used.

4 Conclusions

The data reported in the present study expand on a larger project at NIST providing bubble point, speed of sound, and density data to improve the available models for refrigerant mixtures in REFPROP. The data reported in this study were used to test current mixture models included in REFPROP, which are based on the most recent pure-fluid equations of state [7–11] and available binary interaction parameters [12, 13]. Comparisons of the current REFPROP mixture models for R-125/1234yf and R-1234yf/152a show that only minor adjustments may be needed to provide an accurate representation of the experimental speed of sound data. However, greater adjustments are required to improve the model

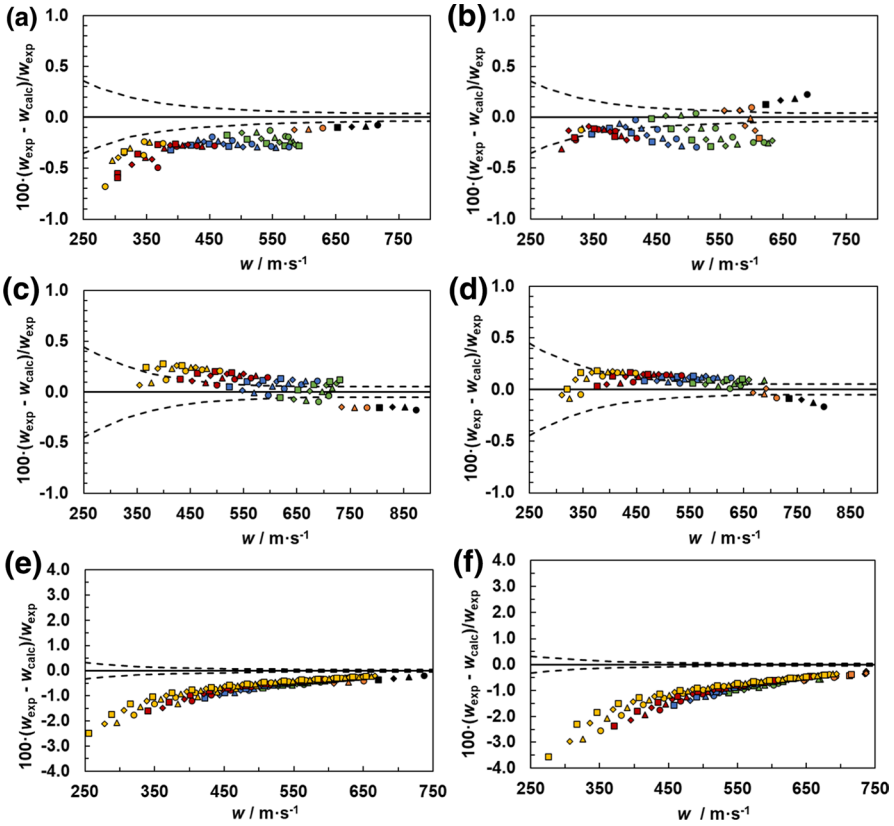

Fig. 2 Deviation graphs comparing experimental speed of sound values, w_{exp}, to speed of sound values calculated using REFPROP [6] mixture models that incorporate pure-fluid EOS [7–11] and fitted binary interaction parameters [12, 13], w_{calc}, as a function of w_{exp}. Dashed lines represent the experimental uncertainty of the speed of sound data as a function of the speed of sound. The systems and molar compositions are (a) R-125/1234yf (0.33351/0.66649), (b) R-125/1234yf (0.66643/0.33357), (c) R-1234yf/152a (0.33342/0.66658), (d) R-1234yf/152a (0.66526/0.33474), (e) R-1234ze(E)/227ea (0.33265/0.66735), and (f) R-1234ze(E)/227ea (0.66803/0.33197). Comparisons are shown at temperatures, ●, 230 K; ▲, 235 K; ◆, 240 K; ■, 245 K; ●, 250 K; ▲, 255 K; ◆, 260 K; ■, 265 K; ●, 270 K; ▲, 275 K; ◆, 280 K; ■, 285 K; ●, 290 K; ▲, 295 K; ◆, 300 K; ■, 305 K; ●, 310 K; ▲, 315 K; ◆, 320 K; ■, 325 K; ●, 330 K; ▲, 335 K; ◆, 340 K; and ■, 345 K (Color figure online)

for the R-1234ze(E)/227ea system, which is currently based on (1) an EOS for pure R-1234ze(E) that requires further adjustments to accurately reflect experimental speed of sound data [5, 14] and (2) binary interaction parameters for the R-1234yf/227ea system [12]. The speed of sound data from the present study along with bubble point and density data from our group will be used to further improve refrigerant mixture models which will be included in future versions of REFPROP.

Table 6 Statistical measures used to evaluate present REFPROP [6] mixture models

Mixture	Composition/ mole frac	Δ_{AAD}/ %	Δ_{bias}/ %	Δ_{max}/ %
R-125/1234yf	(0.33351/0.66649)	0.27	−0.27	0.68
R-125/1234yf	(0.66643/0.33357)	0.15	−0.12	0.31
R-1234yf/152a	(0.33342/0.66658)	0.13	0.08	0.28
R-1234yf/152a	(0.66526/0.33474)	0.10	0.08	0.18
R-1234ze(E)/227ea	(0.33265/0.66735)	0.62	−0.62	2.48
R-1234ze(E)/227ea	(0.66803/0.33197)	0.94	−0.94	3.57

The average absolute deviation (Δ_{AAD}), bias (Δ_{bias}), and maximum deviation (Δ_{max}) defined by Eqs. 1–3 are listed, respectively

Supplementary Information The online version contains supplementary material available at https://doi.org/10.1007/s10765-022-03052-7.

Acknowledgements We thank Megan Harries and Jason Widegren for providing analysis of the pure fluids used to prepare the binary mixtures studied in this work, Stephanie Outcalt for degassing the pure refrigerant samples, Mark McLinden for his guidance in preparing the gas mixtures for the speed of sound measurements and technical discussions pertinent to this work, Ian Bell for his helpful technical discussions pertaining to the Helmholtz-energy-explicit EOS, and Eric Lemmon and Ryo Akasaka for providing the fluid file for the R-1234yf EOS. We gratefully acknowledge the support of the U.S. Department of Energy, Building Technologies Office under Agreement 892434-19-S-EE000031.

References

1. S.L. Outcalt, A.J. Rowane, Bubble point measurements of mixtures of HFO and HFC refrigerants. J Chem Eng Data **66**, 4670–4683 (2021)
2. S.L. Outcalt, A.J. Rowane, Bubble point measurements of three binary mixtures of refrigerants: R-32/1234yf, R-32/1234ze(E), and R-1132a/1234yf. J Chem Eng Data **67**, 932–940 (2022)
3. A.J. Rowane, R.A. Perkins, Speed of sound measurements of binary mixtures of difluoromethane (R-32) with 2,3,3,3-tetrafluoropropene (R-1234yf) or trans-1,3,3,3-tetrafluoropropene (R-1234ze(E)) refrigerants. Int J Thermophys **43**, 46 (2022)
4. A.J. Rowane, R.A. Perkins, Speed of sound measurements of binary mixtures of 1,1,1,2-tetrafluorethane (R-134a), 2,3,3,3-tetrafluoropropene (R-1234yf), and *trans*-1,3,3,3-tetrafluoropropene (R-1234ze(E)) refrigerants. J Chem Eng Data **67**, 1365–1377 (2022)
5. I.H. Bell, Mixture models for R-1234yf/134a, R-1234yf/1234ze(E), and R-134a/1234ze(E) and interim models for R-125/1234yf, R-1234ze(E)/227ea, and R-1234yf/152a. J Phys Chem Ref Data **51**, 013103 (2022)
6. E.W. Lemmon, I.H. Bell, M.L. Huber, M.O. McLinden, *NIST Standard Reference Database 23: Reference Fluid Thermodynamic and Transport Properties-REFPROP, Version 10.0* (Gaithersburg, MD, National Institute of Standards and Technology, 2018)
7. E.W. Lemmon, R. Akasaka, An international standard formulation for 2,3,3,3-tetrafluoroprop-1-ene (R1234yf) covering temperatures from the triple-point temperature to 410 K and pressures up to 100 MPa. Int J Thermophys **43**, 119 (2022). https://doi.org/10.1007/s10765-022-03015-y
8. M. Thol, E.W. Lemmon, Equation of state for thermodynamic properties of *trans*-1,3,3,3-tetrafluoropropene [R-1234ze(E)]. Int J Thermophys **37**, 28 (2016)
9. E.W. Lemmon, R. Span, Thermodynamic properties of R-227ea, R-365mfc, R-115, and R-1311. J Chem Eng Data **60**, 3745–3758 (2015)

10. E.W. Lemmon, R.T. Jacobsen, A new functional form and new fitting techniques for equations of state with application to pentafluoroethane (HFC-125). J Phys Chem Ref Data **34**(1), 69–108 (2005)
11. S.L. Outcalt, M.O. McLinden, A Modified Benedict-Webb-Rubin equation of state for the thermodynamic properties of R-152a (1,1-difluoroethane). J Phys Chem Ref Data **25**, 605 (1996)
12. I.H. Bell, E.W. Lemmon, Automatic fitting of binary interaction parameters for multi-fluid Helmholtz-energy-explicit mixture models. J Chem Eng Data **61**, 3752–3760 (2016)
13. I.H. Bell, D. Riccardi, A. Bazyleva, M.O. McLinden, Survey of data and models for refrigerant mixtures containing halogenated olefins. J Chem Eng Data **66**(6), 2335–2354 (2021)
14. M.O. McLinden, R.A. Perkins, A dual-path pulse echo instrument for speed of sound of liquids and dense gases and measurements on *p*-xylene and four halogenated-olefin refrigerants [R1234yf, R1234ze(E), R1233zd(E), and R1336mzz(Z)]. To be submitted to J Chem Thermodyn (2022)
15. G. L. Harris, *Selected Laboratory and Measurement Practices and Procedures to Support Basic Mass Calibrations (NISTIR 6969)* (National Institute of Standards and Technology, Gaithersburg, MD, 2018)

Authors and Affiliations

Aaron J. Rowane[1] · Richard A. Perkins[1]

✉ Aaron J. Rowane
Aaron.Rowane@nist.gov

[1] Applied Chemicals and Materials Division, National Institute of Standards and Technology, Boulder, CO 80305, USA